Influence of the North Atlantic SST tripole on northwest African rainfall

Shuanglin Li
NOAA-CIRES Climate Diagnostics Center, University of Colorado, Boulder, Colorado, USA

Walter A. Robinson
Department of Atmospheric Sciences, University of Illinois, Urbana, Illinois, USA

Shiling Peng
NOAA-CIRES Climate Diagnostics Center, University of Colorado, Boulder, Colorado, USA

Received 1 November 2002; revised 23 June 2003; accepted 1 August 2003; published 2 October 2003.

[1] The sea-surface temperature (SST) tripole, with warm anomalies off the east coast of the United States and cold anomalies north of 40°N and south of 25°N, is the leading mode of interannual variability in wintertime North Atlantic SST. Its influence on northwest African rainfall is investigated by using a large-ensemble of GCM simulations. Firstly the modeled basin-scale rainfall impact is displayed, and the results suggest: in early-mid winter (November–January), a positive SST tripole causes a reduced rainfall extending from the tropical North Atlantic northeastward to Mediterranean while a negative SST causes a south-north increased rainfall across the central Atlantic from the subtropics to the midlatitude. In late winter (February–April) a positive SST tripole causes a reduced rainfall in the central Atlantic from the subtropics to the midlatitude while a negative SST tripole induces a zonal increased rainfall from the subtropics to Mediterranean. The asymmetry and seasonal dependence of the SST influence on the basin-scale rainfall is consistent with the nonlinear response of the large-scale atmospheric circulation. Under the large-scale impact background, northwest Africa regional rainfall response is also nonlinear and seasonally dependent. In early-mid winter a positive SST tripole causes reduced rainfall, while a negative SST has little effect. In late winter a negative SST tripole induces increased rainfall, while a positive tripole has little effect. A similarly large-scale asymmetric association between SST and rainfall-circulation exists in observations in late winter, while the observed seasonal dependence of this association is relatively weak. Also, a similar SST tripole association with the regional rainfall over the northwest coast of Africa exists in observations. *INDEX TERMS:* 3309 Meteorology and Atmospheric Dynamics: Climatology (1620); 3339 Meteorology and Atmospheric Dynamics: Ocean/atmosphere interactions (0312, 4504); 3354 Meteorology and Atmospheric Dynamics: Precipitation (1854); *KEYWORDS:* SST, rainfall, influence

Citation: Li, S., W. A. Robinson, and S. Peng, Influence of the North Atlantic SST tripole on northwest African rainfall, *J. Geophys. Res.*, *108*(D19), 4594, doi:10.1029/2002JD003130, 2003.

1. Introduction

[2] The northwest coast of Africa is semiarid. Rain occurs only during the winter, and there is a sharp decrease in rainfall rates southward from the Mediterranean and Northern Atlantic coasts. The region is vulnerable to small changes in rainfall. Frequent droughts since the late-1970s have adversely affected agricultural production and water supplies. There is, therefore, interest in understanding the long-term trends and variability in rainfall, and in exploring possible bases for seasonal prediction [*Lamb and Peppler*, 1987; *Lamb et al.*, 1997].

Copyright 2003 by the American Geophysical Union.
0148-0227/03/2002JD003130$09.00

[3] Within this region, it has been shown that variations in Moroccan rainfall are associated with the North Atlantic Oscillation (NAO). Moroccan rainfall is negatively correlated with the NAO index [*Lamb and Peppler*, 1987]. The NAO control of Moroccan precipitation increases steadily from October until January–February, after which it decreases significantly [*Lamb et al.*, 1997]. Although the simultaneous correlation between Moroccan precipitation and the NAO is strong, the relationship between rainfall in one month and the NAO in preceding months is weak and, therefore, of limited use for prediction.

[4] The NAO influences Moroccan rainfall through its modulation of the Atlantic stormtrack. *Rogers* [1990, 1997] demonstrated that when the NAO is positive, enhanced

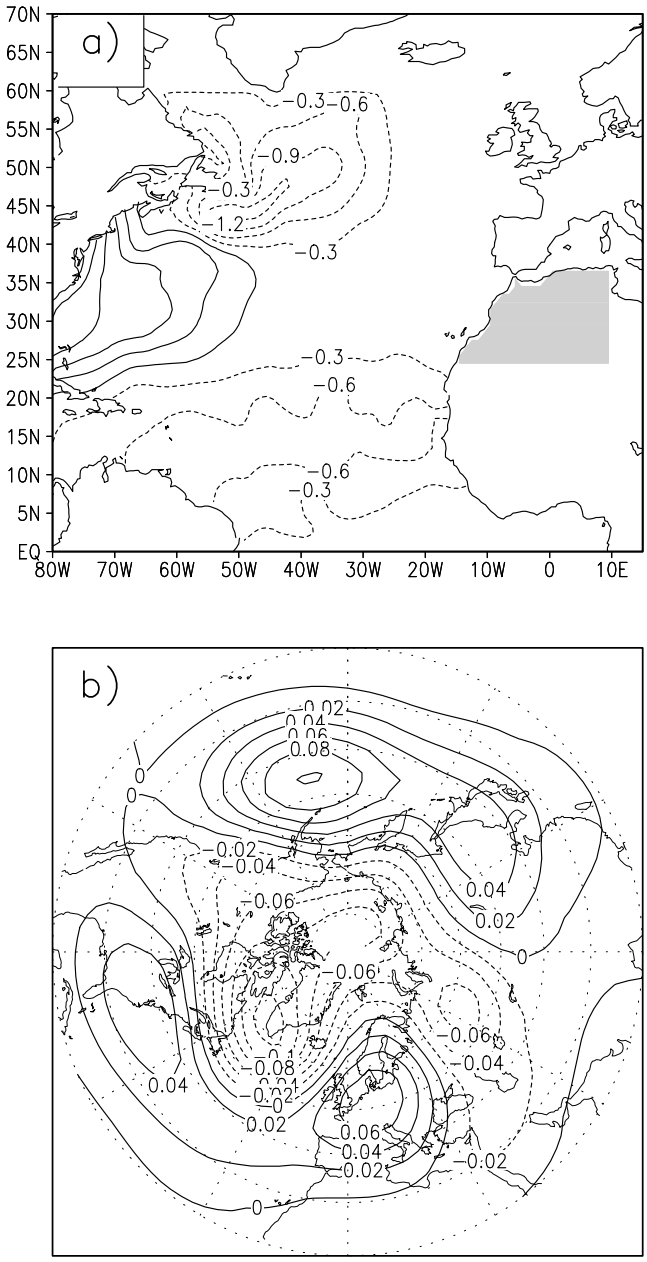

Figure 1. The SST tripole (K) used in the experiments and the leading EOF of observed 500 hPa heights in October–April, which is used to obtain the SST tripole by regression and explains 16% of the total variance. The shaded is the NW Africa region focused in this paper.

midlatitude westerlies steer synoptic-scale eddies further to the north and the east, giving the North Atlantic stormtrack a southwest-northeast orientation that carries synoptic systems and rainfall away from NW Africa. When the NAO is negative, the weakened westerlies make the North Atlantic stormtrack more zonal, and more weather systems reach the coastal region, bringing enhanced rainfall. *Hurrell* [1995] found the same association.

[5] The NAO is the dominant mode of interannual variability of wintertime circulation over the North Atlantic. While it is primarily a dynamical mode of variability internal to the atmosphere (it appears in models with fixed SST [cf. *Ting and Lau*, 1993]), the NAO covaries significantly with the SST tripole (Figure 1), the leading pattern of wintertime SST variability in the North Atlantic. The SST tripole responds to atmospheric forcing associated with the NAO [*Cayan*, 1992a, 1992b], but the tripole itself induces an NAO-like atmospheric response. This has been demonstrated in simulations [*Rodwell et al.*, 1999; *Sutton et al.*, 2001; *Peng et al.*, 2002] and in observations [*Czaja and Frankignoul*, 2002].

[6] In previous papers [*Peng et al.*, 2002, 2003] very large ensembles of general circulation model (GCM) runs were used to determine the influence of the SST tripole on the overlying atmospheric circulation and to explore the dynamics of that response. Here we exploit the large size of these ensembles (100 members each) to investigate whether the previously demonstrated influence of the SST tripole on the atmospheric circulation extends to an influence on NW African rainfall. We address two specific questions: (1) Does our GCM display a significant influence of the SST tripole on NW African rainfall? (2) Is such an influence consistent with SST-rainfall associations deduced from observations?

[7] Any modeled influence of the SST is of interest, only if it arises from physically reasonable and realistic interactions between the large-scale atmospheric circulation and the distribution of precipitation. Therefore, we first investigate whether our model captures the observed connections between the atmosphere internal variability and NW African rainfall.

[8] The paper is organized as follows: Section 2 describes the experiments and analyses, and compares the variability of NW African rainfall among several rainfall data sets. Section 3 discusses the internal atmospheric variability associated with NW African rainfall in our simulations in comparison with observations. Section 4 shows the simulated large-scale responses of the atmosphere to the SST tripole. These are again compared with observations. The simulated response of NW African regional rainfall and its comparison with the observations are described in section 5. A summary and some discussion are provided in the final section.

2. Experiments and Data

[9] Our GCM is a version of the National Centers for Environmental Prediction (NCEP) operational seasonal forecast model, with a T42 spectral truncation and 28 levels [*Peng et al.*, 2002]. Three ensembles of 100-member runs are conducted using climatological seasonally evolving SST (the control runs) and with the tripole SST anomaly (Figure 1) added or subtracted from the climatological SST (the positive/negative tripole runs). The model is integrated for eight months (September–April) starting from 100 different initial conditions taken from the NCEP/NCAR reanalysis from 00Z, Sept. 1–5, 1980–1999 [*Kalnay*, 1996]. These runs form the 100 members of each ensemble. Monthly mean values of geopotential heights and winds on a $2.5^\circ \times 2.5^\circ$ grid and precipitation rates and surface pressure on the T42 Gaussian grid are obtained from the twice-daily model output. The monthly rainfall response is derived from the difference between the ensemble averages for each month. A seasonal response is obtained from 3-month average of the monthly responses. For early-mid winter, this

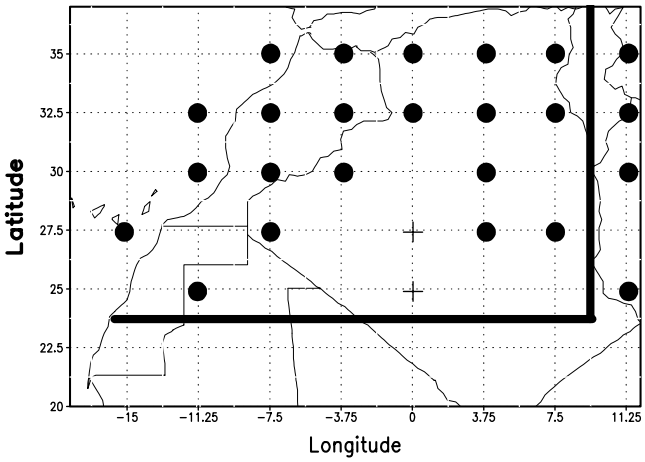

Figure 2. The grid points (denoted by solid circles) over northwest Africa with rainfall available in Hulme's global land-area precipitation data set. The two points denoted by pluses have rainfall available only in some years, and thus are not included in calculating the rainfall index.

is the average from November through January, whereas for late winter it is the average from February through April.

[10] The SST tripole used in the experiments is determined by regressing the observed global SST on the principal component time series of the leading empirical orthogonal function (EOF) of Northern Hemisphere 500 hPa monthly-mean October–April geopotential heights [*Peng et al.*, 2002]. Monthly 500 hPa heights for 1948–2000 from the NCEP/NCAR reanalysis and monthly SST for 1948–1998 from the GISST data set [*Rayner et al.*, 1996] are used. The leading EOF of wintertime 500 hPA height features an NAO-like dipole over the North Atlantic. The principal component time series for this pattern is strongly correlated with a typical NAO index denoted by sea surface pressure difference between Lisbon of Portugal and Iceland [*Rogers*, 1984], with a correlation coefficient greater than 0.8. The SST pattern obtained by regression against this principal component time series closely resembles that obtained by regressing the SST on the NAO index. Both are dominated by a tripole pattern in the North Atlantic, and the two patterns have a spatial correlation coefficient of 0.81. Thus, our SST tripole pattern is linearly related to the NAO. This SST tripole pattern is amplified to have a maximum strength of 1.2K (Figure 1).

[11] To illustrate the relationship between observed NW African precipitation and the atmospheric circulation, we use monthly mean data for 1948–2000 from the NCEP/NCAR reanalysis. Geopotential heights, Z, horizontal winds, u and v, and vertical velocities, ω, at 17 vertical pressure levels are taken from the 2.5° × 2.5° latitude-longitude grid, and monthly precipitation rates are taken from T63 Gaussian grids. To verify the reanalysis precipitation data and to evaluate the ability of the model in simulating the rainfall climatology of NW Africa, we use global land-area monthly precipitation data, gridded at 2.5° latitude by 3.75° longitude, from 1900–1998 [*Hulme*, 1992], and global monthly precipitation data obtained by merging gauge, satellite and numerical model predictions, gridded at 2.5° latitude by 2.5° longitude, from 1979–2002 [*Xie and Arkin*, 1997]. These two data sets are denoted Hulme's rainfall and Xie's rainfall. Not all land grids have values in Hulme's rainfall data, and Figure 2 displays the NW African grid points where values are available. Because the Hulme's rainfall value over a grid is estimated from land station observed rainfall within the grid box, the values over several grids off shore represent observed rainfall of the coastal land or island stations within the grid box [*Hulme*, 1992]. The time series of monthly rainfall anomalies for 17 Moroccan coastal stations from 1948–1999 [*Ward et al.*, 1999] are used to supplement the precipitation data. Below we compare these precipitation data, together with the model rainfall, in describing the variability of NW African rainfall.

[12] A monthly comparison of the model's ensemble averaged rainfall in winter (September to April) with other rainfall data sets shows that the model captures the large-scale distribution and seasonal march of rainfall. NW Africa is at the southern edge of the North Atlantic rainfall belt, which has a southwest-northeast orientation and a maximum over the central North Atlantic, southeast of Newfoundland, immediately south of the Atlantic stormtrack. This suggests that NW African rainfall is controlled primarily by the southeast end of the Atlantic rainfall belt associated with the stormtrack. Starting in September, the Atlantic rainfall belt begins to move southward. NW African rainfall increases, reaches its peak around December, and then decreases gradually, becoming very weak by summer. Figure 3 shows the model's rainfall in the vicinity of NW Africa in early-mid winter and in late winter, together with that from other data sets. Rainfall over NW Africa falls mainly along the Atlantic and Mediterranean coasts and decreases rapidly inland, in both the model and the other data sets. Rainfall in Morocco and northern Algeria, therefore, comprises a dominant portion of NW African rainfall. In early-mid winter (Figures 3a, 3c, 3e, and 3g), the inland decrease of precipitation in the model is gentler than that in the observations, but the most rapid decrease still occurs in Morocco and northern Algeria, which is largely consistent with the other data sets. In late winter (Figures 3b, 3d, 3f, and 3h), the model's rainfall distribution agrees well with the observations, even in its details. This indicates that the model captures the main features of the climatological distribution of NW Africa rainfall in early-mid winter and in late winter.

[13] The strength of NW African rainfall is described using a precipitation index defined as the mean of the precipitation rate over all data grid points within the region (the shaded area in Figure 1). For the model rainfall, the reanalysis, Xie's data, and Hulme's data, the rainfall index is the mean of 29, 67, 38 and 16 data points, respectively over their grids. Figure 4 displays the seasonal march of the rainfall index. Coastal Morocco contributes a substantial portion of NW African rainfall (Figure 3). For comparison, the seasonal march of observed coastal Moroccan rainfall, derived from the mean of 1933–1983 gauge rainfall in five coastal stations [see *Lamb and Peppler*, 1987, Figure 4], is also displayed together (Figure 4e). Rainfall in the model increases rapidly from a weak value in September to a much large value in November, and decreases gradually after January, consistent with both Hulme's and Xie's data. The model rainfall, however, peaks in November, one month ahead of the observations. Both the model and the reanalysis rainfall are weaker than Hulme's and Xie's values. For

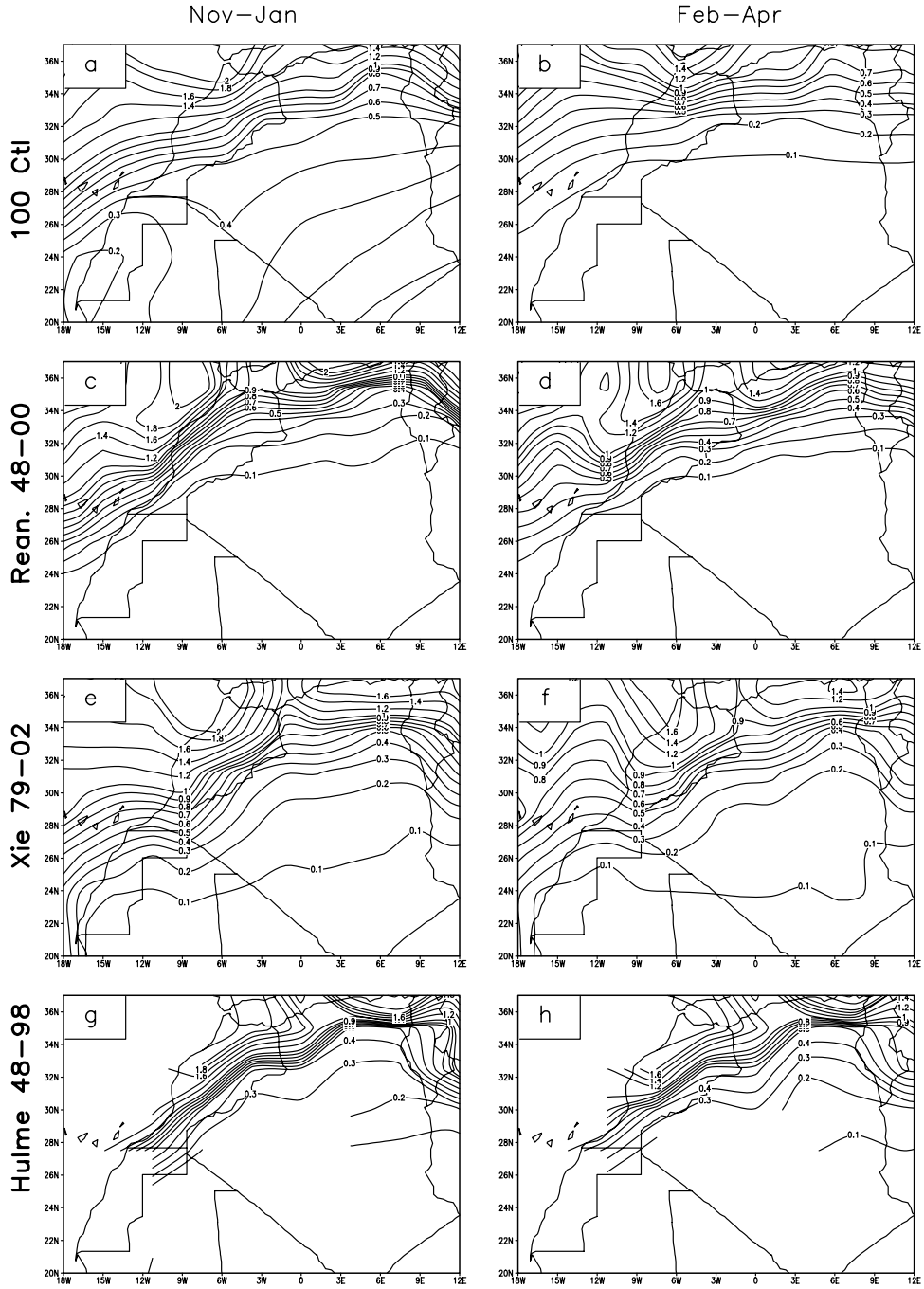

Figure 3. Distribution of precipitation (mm/day) over northwest Africa in early-mid winter (left panel) and late winter (right panel). (a)(b) for the GCM, (c)(d) for the NCEP/NCAR reanalysis, (e)(f) for Xie's global precipitation, and (g)(h) for Hulme's global land-area rainfall.

example, the wintertime (October–April) mean is greater than 0.5 mm/day in both Hulme's and Xie's data, compared with only around 0.4 and 0.2 in the model and the reanalysis. In addition, the reanalysis rainfall peaks in April, much later than in the other data sets. All these rainfall data sets, however, show a rainy season in the winter half year and a very dry summer. Coastal Moroccan rainfall also has a similar seasonal cycle to that in NW Africa.

[14] Figure 5 displays the observed interannual evolution of NW African rainfall. In both early-mid and late winter, the year-to-year variations in these rainfall data are in mutual agreement. The different data sets display nearly the same extreme wet and dry years. The correlations between these indexes are significant, with coefficient values of 0.62 and 0.65 in early-mid and late winter between the reanalysis and Hulme's rainfall from 1949–1998, and greater correlation coefficient values between them and with Xie's rainfall from 1979–1998.

[15] Judging from the spatial distribution of rainfall, its seasonal march and its interannual evolution, the reanalysis

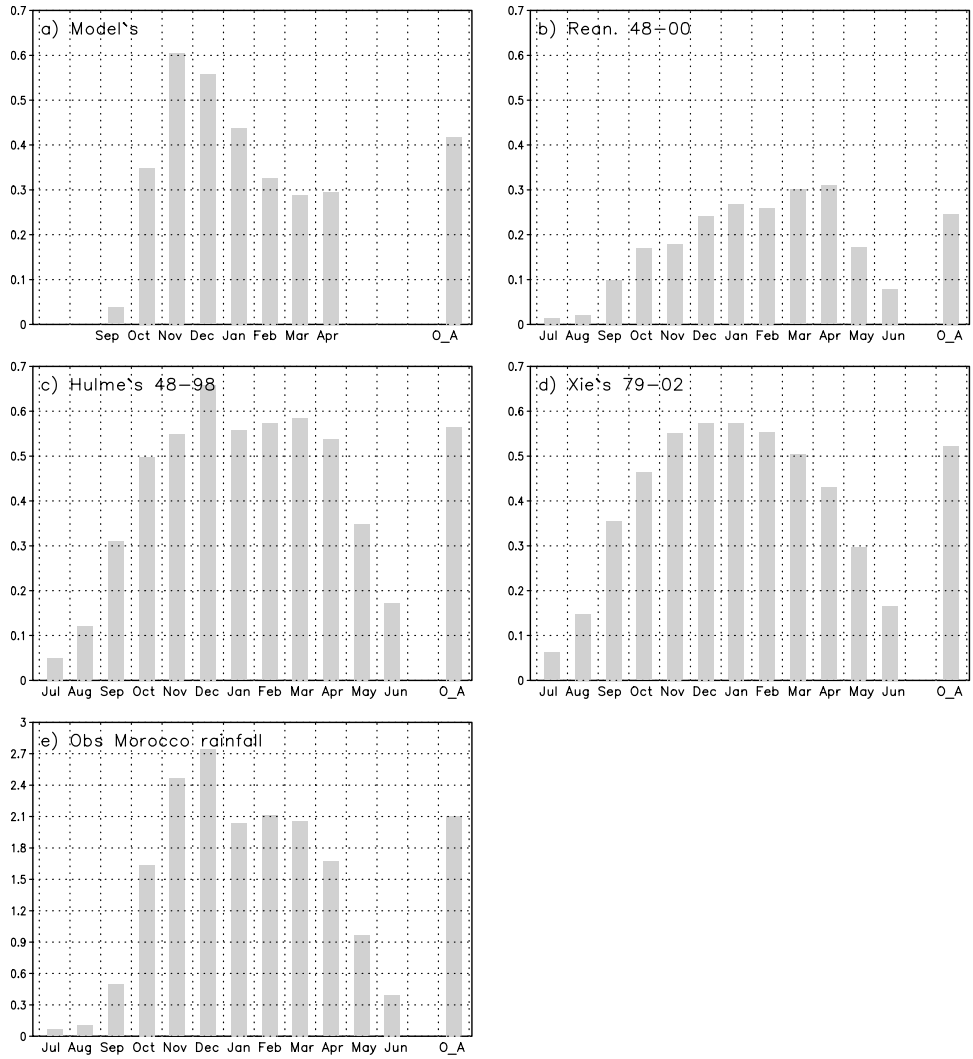

Figure 4. Climatological seasonal march of northwest African precipitation (mm/day) from (a) the GCM control run, (b) NCEP/NCAR reanalysis, (c) Xie's rainfall data set, and (d) Humle's rainfall data set. For comparison, seasonal march of observed coastal Morocco rainfall derived from *Lamb and Peppler* [1987] is displayed in (e).

captures the main characteristics of NW African rainfall, thus is appropriate for identifying dry and wet events, to be used for determining the associated large-scale circulation.

3. Observed and Simulated Internal Variability Associated With NW Africa Precipitation Anomalies

[16] Here we use composites of months with extreme rainfall to address whether our model captures the circulation anomalies that are associated with NW African rainfall in nature. Months with NW African precipitation index 65% greater or less than its mean value are selected to represent the wettest and driest conditions. Using this criterion, we have 26 (28) wet (dry) months for early-mid winter and 27 (22) wet (dry) months for late winter out of the 159 early-mid winter or late winter months within the reanalysis period, 1948–2000.

[17] Figure 6 displays composites of the reanalysis precipitation rate, 500 hPa band-pass streamfunction variance (to represent the storm track), 500 hPa geopotential height, and 700 hPa pressure vertical velocity for the wettest and driest months during early-mid winter. The band-pass streamfunction is calculated from the transient components of the horizontal wind, obtained using a 61-point temporal filter that extracts 3–10 day periods. NW African rainfall anomalies are associated with large-scale rainfall anomalies across the North Atlantic and Europe. When NW Africa is wet (Figures 6a, 6c, 6e, and 6g), the central North Atlantic is dry. There are negative 500 hPa height anomalies and increased synoptic-eddy activity over NW Africa, and positive height anomalies and reduced synoptic-wave activity over the central North Atlantic. These anomalies reflect a southward shift of the eastern end of the North Atlantic stormtrack, which corresponds to the second mode of Atlantic stormtrack variability described by *Rogers* [1997]. When NW Africa is dry, the region of reduced rainfall stretches westward and eastward from coastal NW Africa. Accompanying the reduced rainfall is a large scale zonal belt of enhanced precipitation across the northern

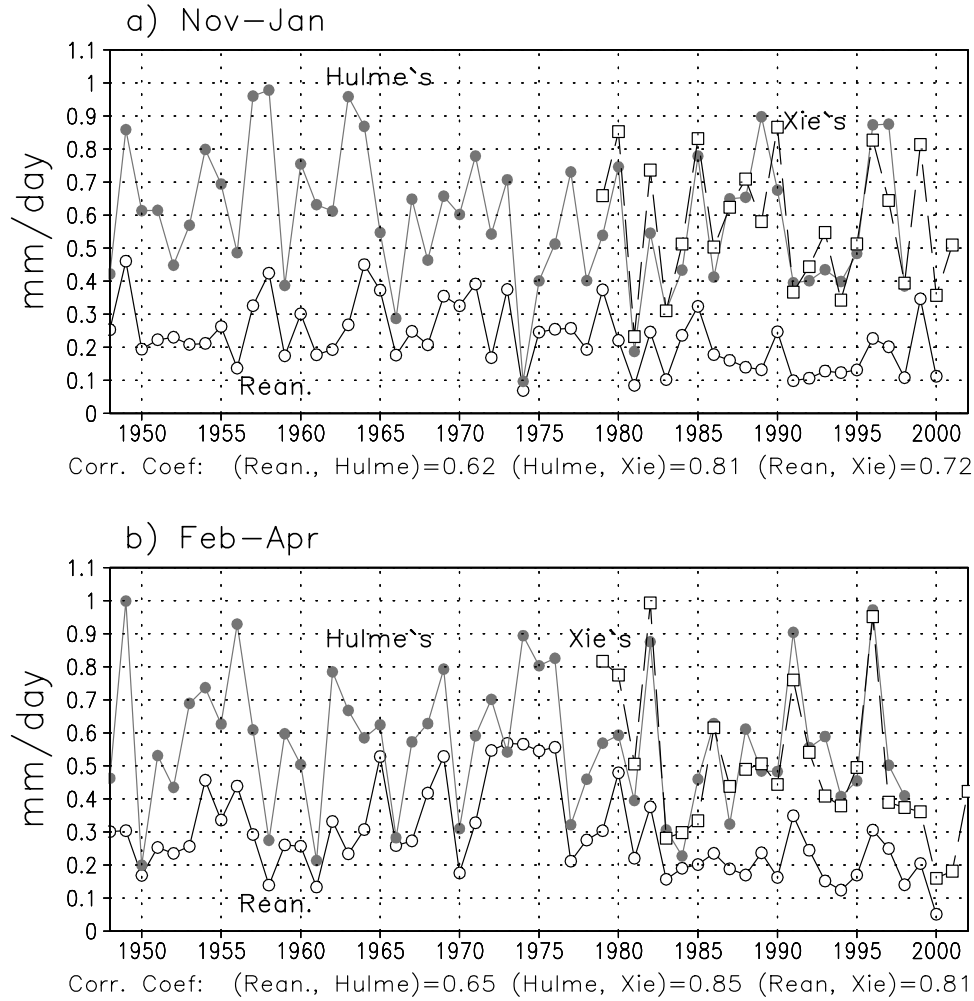

Figure 5. Interannual evolution of northwest African precipitation (mm/day) in early-mid winter (a) and in late winter (b).

North Atlantic and northern Europe. Correspondingly, there is a dipole-like 500 hPa height anomaly along the eastern boundary of the North Atlantic, with a strong positive anomaly and reduced synoptic-eddy activity over NW Africa. These anomalies reflect a southwest-northeast oriented North Atlantic stormtrack, corresponding to one phase of *Rogers*' [1997] first mode of North Atlantic stormtrack variability.

[18] There are asymmetries between the circulation anomaly patterns when NW Africa is wet and dry. The most negative rainfall anomalies when NW Africa is wet are over the central North Atlantic, while the strongest positive rainfall anomalies when NW Africa is dry are over coastal North Europe. This asymmetry is also reflected in the 500 hPa height composites.

[19] The greatest rainfall anomalies do not overlap the strongest anomalies in synoptic-eddy activity for either wet or dry conditions in NW Africa. This suggests that the displacement of baroclinic eddies associated with the stormtrack anomalies is not directly responsible for the rainfall anomalies. The secondary circulation associated with these stormtrack anomalies, however, may explain the rainfall anomalies. The 700 hPa vertical velocities, ω, directly correspond to the rainfall anomalies in both the wet and the dry composites.

[20] Now we turn to the circulation anomalies associated with NW African rainfall anomalies in the GCM. Using the same criterion as above, we have 47 (45) wet (dry) months for early-mid winter and 60 (76) wet (dry) months for late winter out of the 300 possible months for each season of the control ensemble. These composites are computed as for the observations. The only difference is that a "poor man's filter" is used to obtain the synoptic components (timescales less than 9 days) of the winds. A similar filter was used by *Palmer and Sun* [1985], and a test shows no significant differences with the 61-point filter used for the observations.

[21] NW African rainfall and its associated circulation anomalies (Figure 7) are largely consistent with the observations, though the rainfall anomalies are shifted slightly southward in comparison with the observations. This is consistent with the relatively slow inland decrease of precipitation in the model, in comparison with the reanalysis (Figures 3a and 3b). When NW Africa is wet, there is a negative 500 hPa height anomaly and ascending motion at 700 hPa over the maximum rainfall anomaly, and vice versa

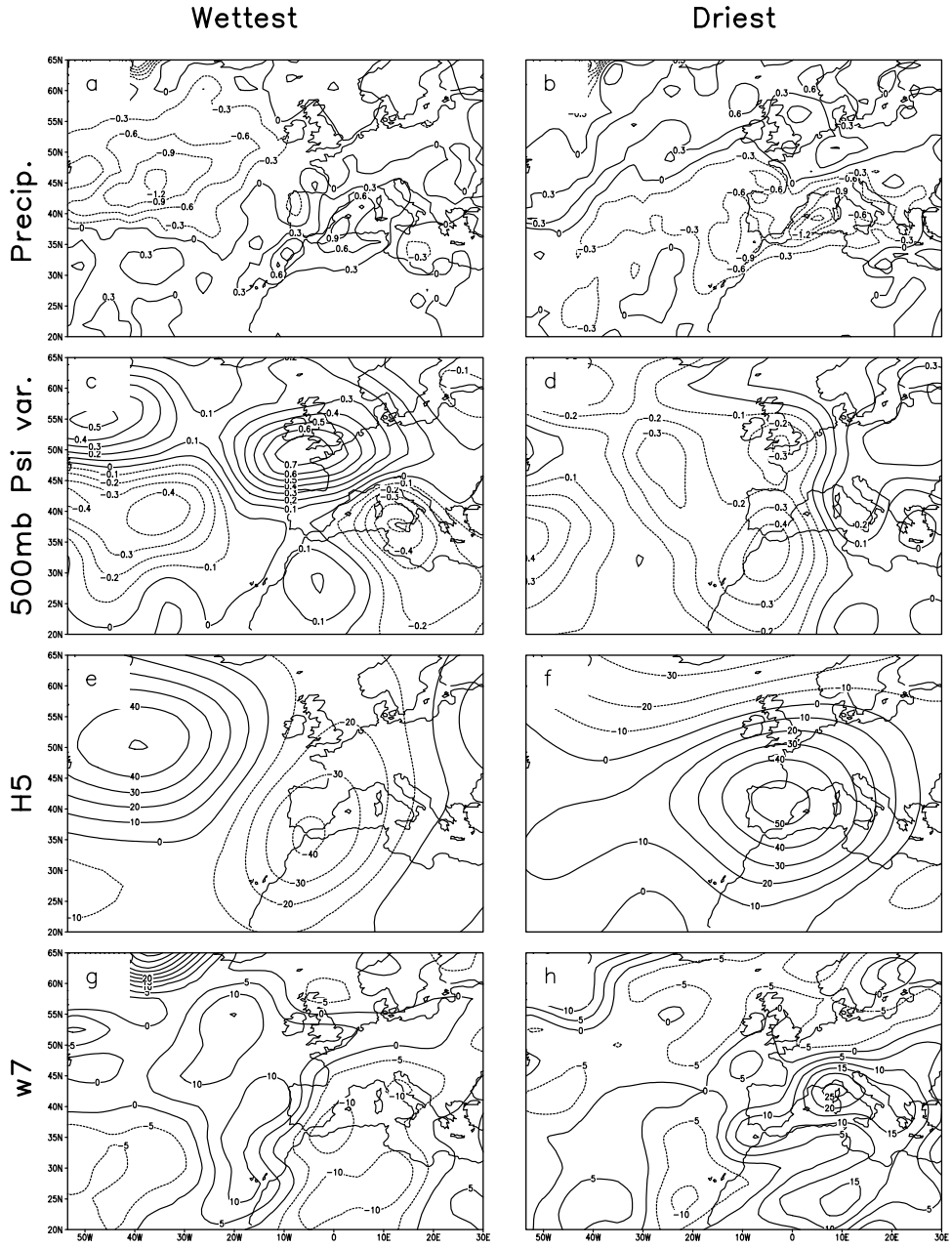

Figure 6. Composites of anomalous precipitation rate (mm/day), 500 hPa transient stream function variance (unit: 10^{13} m^2 s^{-2}), 500 hPa geopotential height (m) and 700 hPa vertical velocity (10^{-3} Pa s^{-1}) for the 26 wettest (a, c, e, g) and 28 driest (b, d, f, h) early-mid winter months in the 1948–2000 NCEP/NCAR reanalysis.

for the dry composite. The stormtrack anomaly is displaced from the rainfall anomaly, as was found in the observations. There is a difference from the observations, however, in that the circulation anomalies in the model are nearly symmetric between the wet and dry composites.

[22] In late winter (Figures 8 and 9), observational rainfall and circulation composites strongly resemble those from the model, and the circulation anomalies from the wet and dry composites are symmetric in both the observations and the simulations. It appears that the model captures the atmospheric internal variability associated with NW African rainfall anomalies better in late winter than in early-mid winter. This is in agreement with the previous result that the observed low- frequency pattern is not well represented by the model in early-mid winter [*Peng et al.*, 2002].

[23] The wettest and driest months used for the observational composites above are derived from the NCEP/NCAR reanalysis. The rainfall anomaly composites for these wet (dry) months using Hulme's data set suggest consistently more (less) rainfall compared with the reanalysis. Given that Moroccan precipitation makes a large contribution to NW African rainfall, similar composites are constructed for the wettest and driest Novembers and Februaries for Morocco.

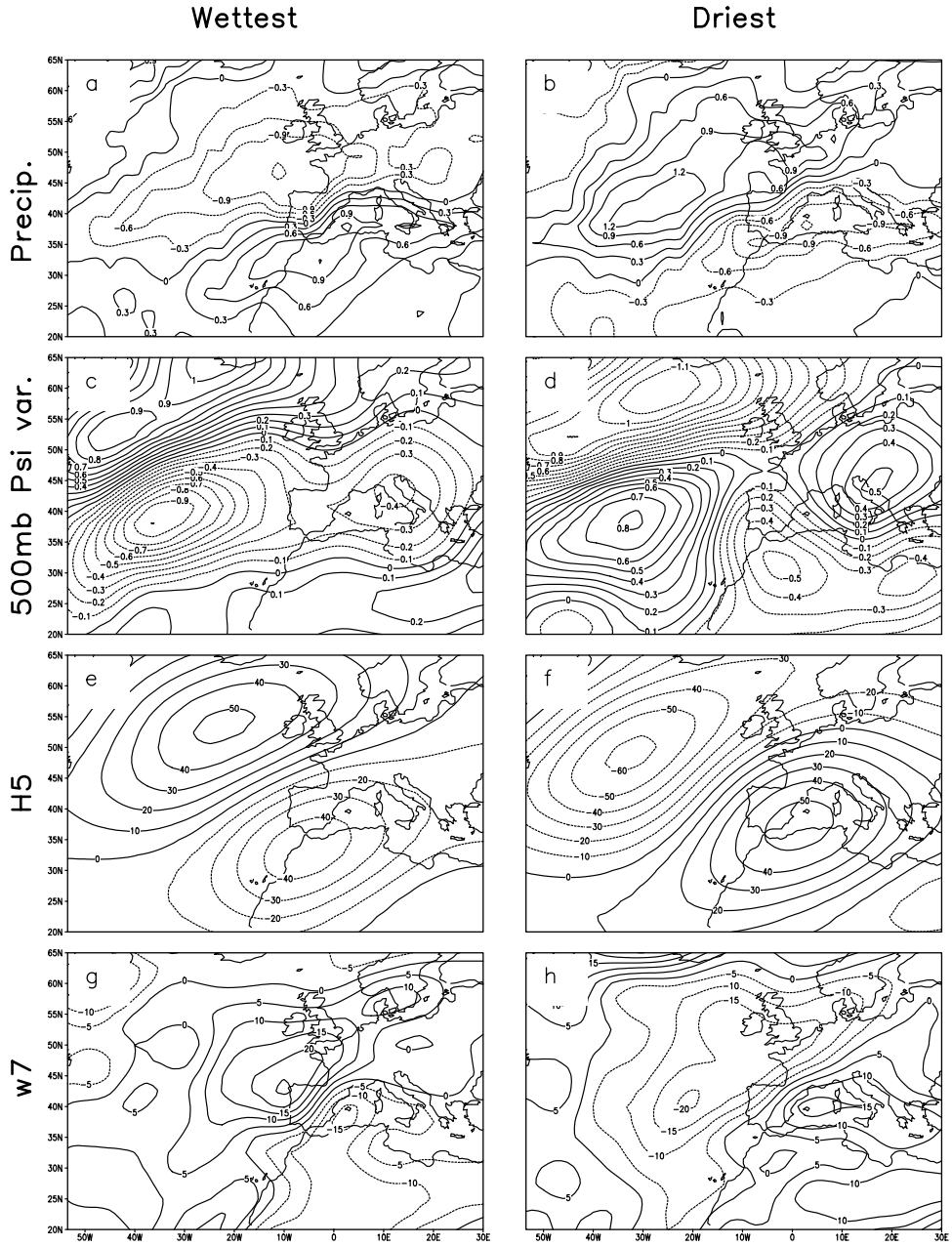

Figure 7. Same as Figure 6, but for the 47 wettest and 45 driest early-mid winter months in the 100 control runs.

The observed Moroccan rainfall is derived from the time-series of 1946–1998 Moroccan station rainfall [*Ward et al.*, 1999]. The rainfall and circulation anomalies in these composites (not shown) resemble that based on the NCEP/NCAR reanalysis rainfall data to some extent, confirming that the model captures the association of circulation anomalies with NW Africa rainfall anomaly described above.

4. Large-Scale Response to the SST Tripole

[24] The large-scale atmospheric response to SST anomalies creates the context in which regional precipitation anomalies develop. In this section we consider this large-scale response, before considering the local response over NW Africa in section 5.

4.1. Simulated Response

[25] Figure 10 displays the simulated response of precipitation to the SST tripole. In early-mid winter, the positive SST tripole induces reduced rainfall over the subtropical eastern North Atlantic and over NW Africa (Figure 10a). For the negative SST tripole (Figure 10b), there is a large region of increased rainfall, extending northward from the subtropical Atlantic to midlatitudes, but there is no significant rainfall anomaly over NW Africa. In late winter, the positive tripole induces a large negative anomaly in rainfall over the central North Atlantic and a small positive anomaly

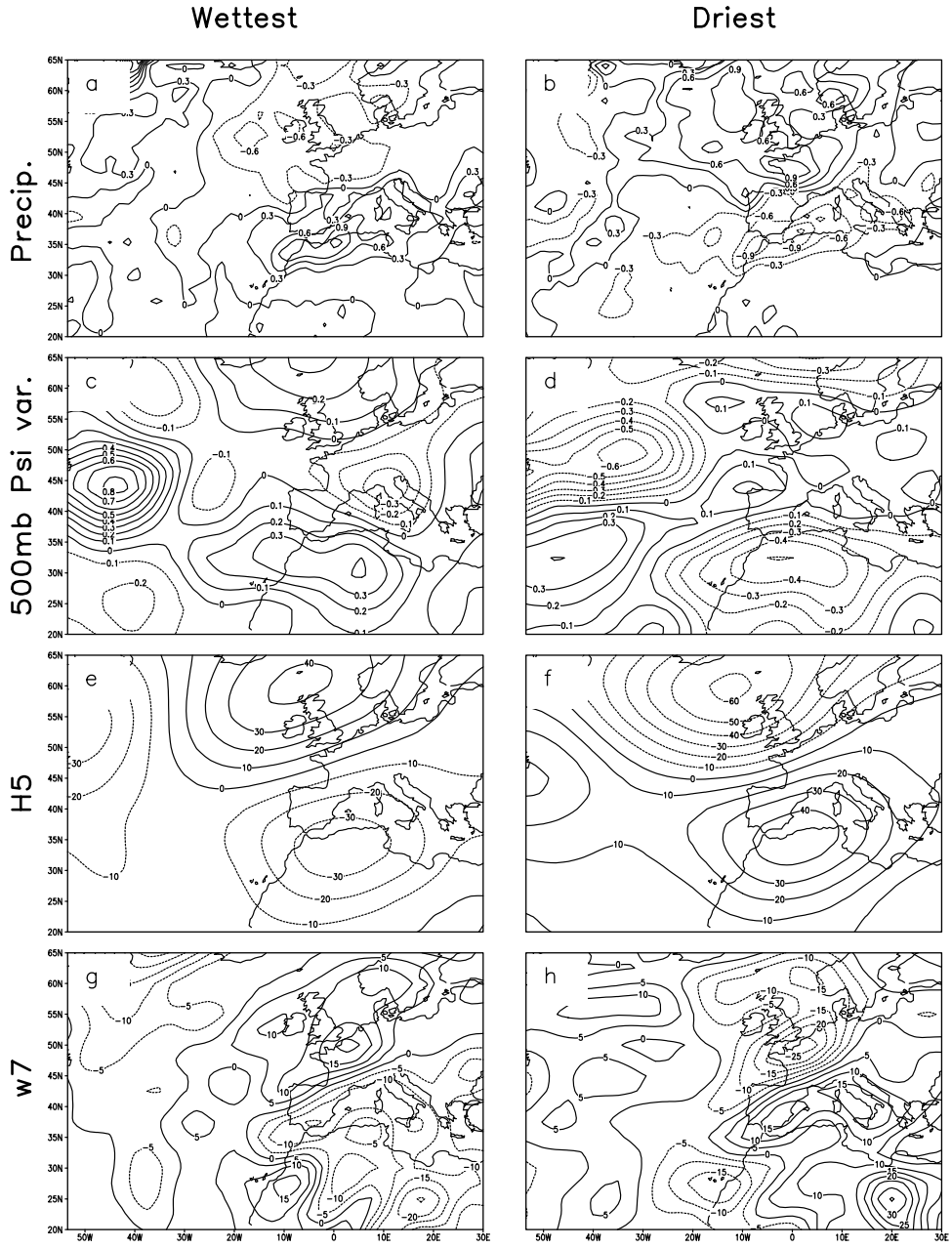

Figure 8. Same as Figure 6, but for the 27 wettest and 22 driest late winter months in the 1948–2000 NCEP/NCAR reanalysis.

to its northeast (Figure 10c), but, again, the NW African rainfall response is not significant. The negative tripole in late winter induces a nearly zonal region of increased rainfall along 35°N. In this case NW Africa is at the southern edge of this wet belt, and it has significantly more rainfall. Thus the simulated broad-scale rainfall response to the SST tripole is nonlinear and seasonal-dependent. Most noteworthy, however, is the fact that only the negative tripole in late winter produces a significantly more rainfall over NW Africa and only the positive tripole in early-mid winter induces a significantly less rainfall.

[26] Figure 11 shows 500 hPa geopotential height responses to the tripole. These clearly exhibit an asymmetry between the responses to the positive and to the negative tripole, as described by *Peng et al.* [2002, 2003]. In early-mid winter (Figures 11a and 11b), the positive SST tripole induces a weak dipole over the eastern North Atlantic, with a positive anomaly west of the Straits of Gibraltar and a stronger negative anomaly centered west of Britain. The 500 hPa height response to the negative tripole is very different, with a negative anomaly over Eastern Europe and a weak positive anomaly across the Sahara.

[27] In late winter (Figures 11c and 11d) the positive tripole induces a wave-train-like height anomaly, with no significant response over the Mediterranean or Africa, consistent with the absence of a significant rain anomaly over NW Africa (Figure 10c). In contrast, the negative tripole induces a dipolar response, with a zonally elongated

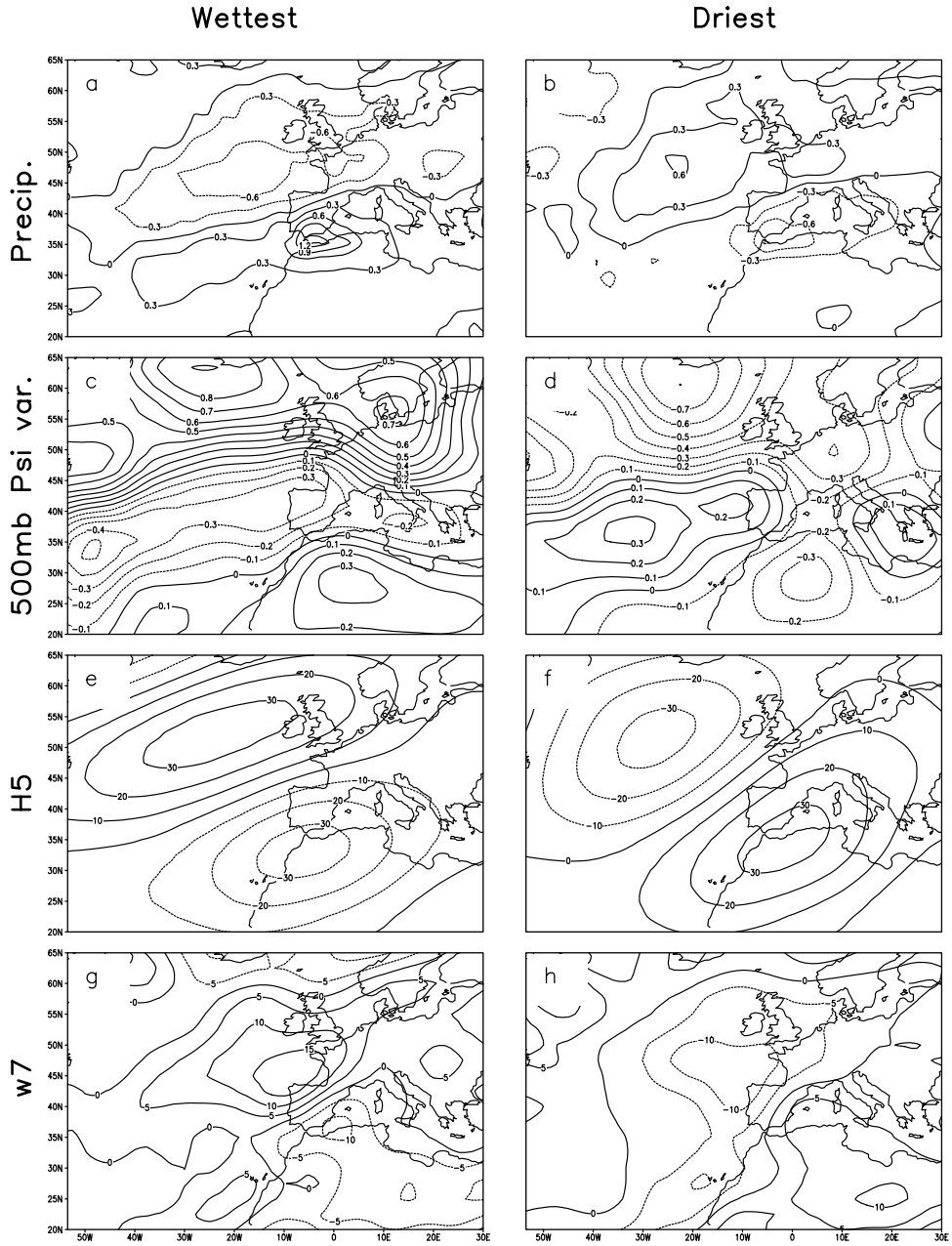

Figure 9. Same as Figure 6, but for the 60 wettest and 76 driest late winter months in the 100 control runs.

negative anomaly, extending from the east coast of North America to southern Europe, and a positive anomaly centered southeast of Greenland, a strong negative projection on the NAO. This pattern is in agreement with the zonally elongated belt of increased rain and the increase in NW African rainfall (Figure 10d) in this case. The height response in late winter is stronger than in early-mid winter, and stronger for the negative than for the positive tripole. Overall, the height response demonstrates the same asymmetry with respect to sign and the same seasonal-dependence, as does the rainfall response.

4.2. Observed Anomalies Associated With the SST Tripole

[28] For comparison with the model responses to SST anomalies, we calculate composites of rainfall and 500 hPa height for months when the observed SST has a strong positive or negative projection on the tripole. When calculating the projection coefficient, grid points over the extratropics (mainly over the extratropical dipole part composing of the SST tripole in Figure 1) are weighted by a factor of three. The derived SST composite using this weighting is more similar to the tripole than without it. Normalized projection coefficients greater than a threshold (or less than the same threshold with reversed sign) are used to define months with strongly positive and negative projections. This threshold is set at 0.5. At this value there are 48 (45) and 55 (58) months with strong positive (negative) projections on the tripole pattern in early-mid and in late winter, both of which are about one third in the total 159 months in each season from 1946–1998. Examining the distribution of the months with

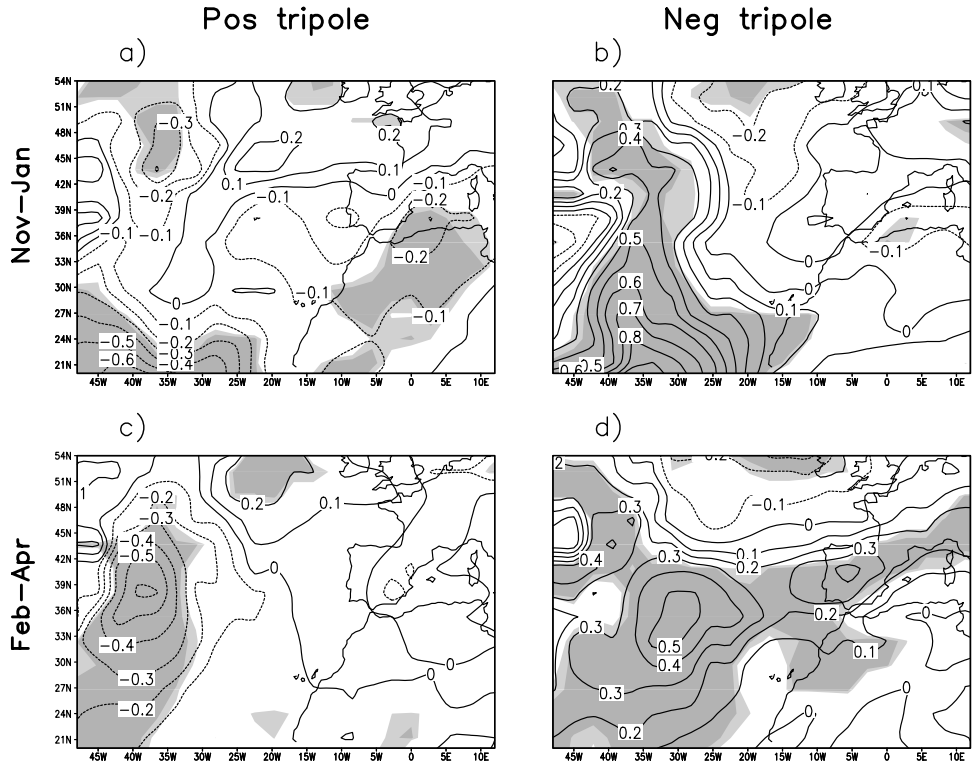

Figure 10. Precipitation response (mm/day) to the SST tripole in a broad-scale section including northwest Africa. (a) To the positive SST tripole in early-mid winter; (b) same as (a) but to the negative tripole; (c) to the positive tripole in late winter; (d) same as (c) but to the negative tripole. The light and dense shadings denote response areas with the significances at the 90% and 95% levels, as estimated by a t-test.

strongly anomalous SST tripole, it is found that there are more years in which two or all three months have the same sign anomaly, than that would be expected by chance. This suggests that there is month-to-month persistence of the SST anomaly. We ignore the persistence and deal each month as an independent sample when conducting significance t-test for the composite difference in the months to the other months. The months of a given signed anomaly are also found to cluster in particular decades, indicating the presence of interdecadal variability in the SST tripole.

[29] Before using these months to construct composites, we verify that there are no significant SST signals, other than the tripole in these months. Otherwise, the composites could reflect atmospheric anomalies associated with other SST patterns. For this purpose, we calculate the composite SST anomalies for these months. The results (not shown) indicate that the strongest SST signal is, indeed, the tripole for all these months, although there is a weakly positive SST anomaly over the tropical eastern Pacific for the negative projection months in late winter, with its value half that of over the subtropical North Atlantic. To further address whether these months include an ENSO signal, we check the possible clustering of ENSO events in these negative projection months in late winter, using the Climate Prediction Center's seasonal ENSO index from 1950 to the present (The CPC's seasonal ENSO index is downloaded via the web site: http://www.cpc.noaa.gov:80/products/analysis_monitoring/ensostuff/ensoyears.htm). The numbers of ENSO, normal and anti-ENSO months are 14, 35, 9, among the 58 negative-projection months in late winter. This indicates that the ENSO signal is not evident in these months. Therefore, the composite reveals the atmospheric anomalies associated with the Atlantic tripole pattern.

[30] Because Xie's data have a short record, and Hulme's data are available only over land, neither data set is appropriate for constructing a composite of the large-scale rainfall anomalies associated with the SST tripole during the period 1948–1998. Instead, the global precipitation in the reanalysis is used here. Figure 12 displays the composites of rainfall anomalies. Two features of these composites are notable. First, in distinct contrast to the model composites, the rainfall anomalies associated with the positive and negative SST tripole are similar in early-mid and late winter. Secondly, the rainfall anomalies associated with the negative tripole are more robust, both in magnitude and in spatial extent. In both seasons, a negative projection on the tripole (Figures 12b and 12d) is associated with a zonal band of enhanced rainfall extending across the subtropical Atlantic, and touching the NW coast of Africa. This pattern is very similar to the late winter response to the negative tripole in the model. The rainfall anomalies associated with the positive tripole (Figures 12a and 12c) show a north-south dipole in the central Atlantic, with increased rainfall in mid latitudes and reduced rainfall in the tropics, which bears some resemblance to the model's response to the positive tripole.

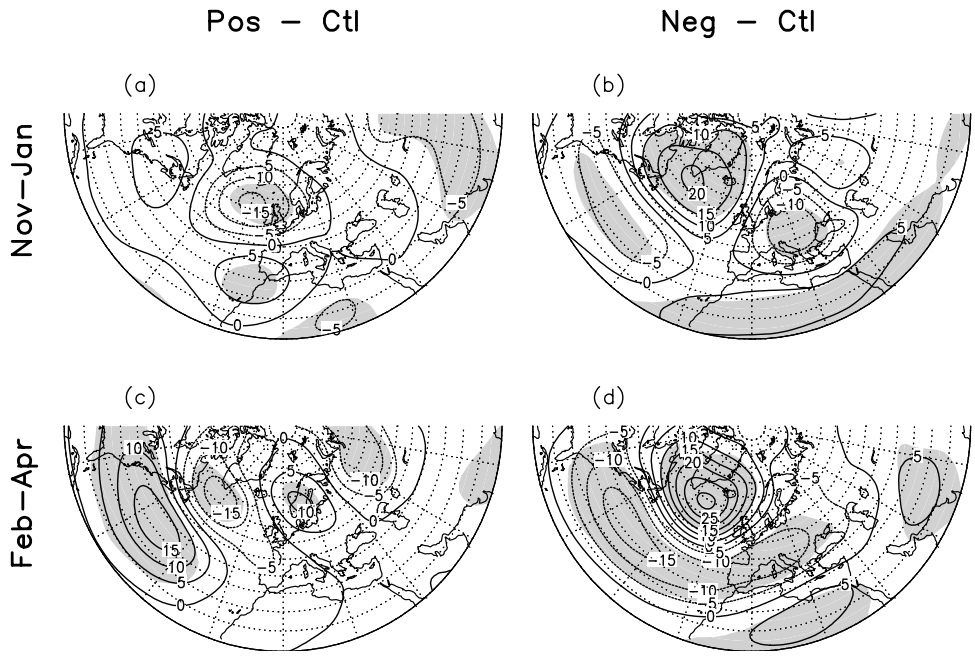

Figure 11. Same as Figure 10, but for 500 hPa geopotential height (m). The shadings denote areas with the response significance at the 95% level, as estimated by a t-test.

[31] Figure 13 displays the observed composite 500 hPa heights. As for the rainfall, the height composites show a more robust association with the SST tripole when the tripole is negative, and they are similar between early-mid and late winter. Also, as for the rainfall, the resemblance between the observed composites and the modeled response to the tripole is much greater in late than in early-mid winter. In both seasons, the elongated subtropical ridge associated with the negative tripole implies a southward shift of the jet and storm track, consistent with the rainfall anomalies shown in Figures 12b and 12d.

5. NW African Regional Rainfall Responses to the SST Tripole

[32] Now we examine the regional response of NW African rainfall to the SST tripole. During early-mid winter, in the presence of the positive SST tripole (Figure 10), the model produces significantly less rainfall over NW Africa. The principal response to the negative tripole is an increase in rainfall over the eastern Atlantic. Thus, the responses to the positive and negative tripole are not complementary. This asymmetry is also evident during late winter. For the positive tripole, there is no significant precipitation response over NW Africa, while for the negative tripole, there is an increase in rainfall over the northwest portion of the region. The nonlinear and seasonally dependent rainfall responses are also reflected in NW Africa rainfall index, which will be discussed later.

[33] From the reanalysis rainfall composite (Figure 12), NW Africa is at the edge of large-scale rainfall belt, and the rainfall response is not as clear as in the GCM simulations. The simulations and the reanalysis are broadly consistent in their rainfall responses for the positive tripole in early-mid winter and the negative tripole in late winter. For example, corresponding to the significant less/more rainfall in the GCM (Figures 10a and 10d), there is a less/more rainfall, though with a weak significance, in the reanalysis near the NW African coast (Figures 12a and 12d). However, evidently, there is inconsistence for the other two situations (compare Figures 10b and 10c with Figures 12b and 12c), especially for the positive SST tripole in late winter, in which there is not significant response in the GCM while a more rainfall extending from Portugal Peninsula in the reanalysis.

[34] Figure 14 shows similar rainfall composite, constructed using Hulme's data. Here, 4 more data grid points off the shore are included, in view of that the values over the grids represent the coastal land rainfall. In comparison with the reanalysis, Hulme's data are more consistent with the simulations, for the positive tripole in early-mid winter and the negative tripole in late winter, especially along the Atlantic coast, as can be seen by comparing Figures 14a and 14d with Figures 10a and 10d. That the observed rainfall anomaly area is smaller than that in the GCM is understandable, given the inability of the GCM to resolve complicated small-scale topography. For the negative tripole in early-mid winter and the positive tripole in late winter, the simulations are not consistent with the observed composite using Hulme's data. This is similar to what is found using observed composites based on the reanalysis.

[35] Figures 15a and 15b display NW African monthly precipitation index, defined as in section 2 but with above 4 more grid points included for Hulme's data, and its seasonal mean for the two seasons for different SST anomalies in the GCM simulations and in Hulme's data set. For comparison, coastal Moroccan rainfall denoted by the mean of the 7 Atlantic coastal grids in Hulme's data set (see Figure 2) is displayed in Figure 15c. In the GCM simulations (Figure 15a), during the early-mid winter months, there is less precipitation in the positive tripole runs in comparison with the control runs, while the difference between the

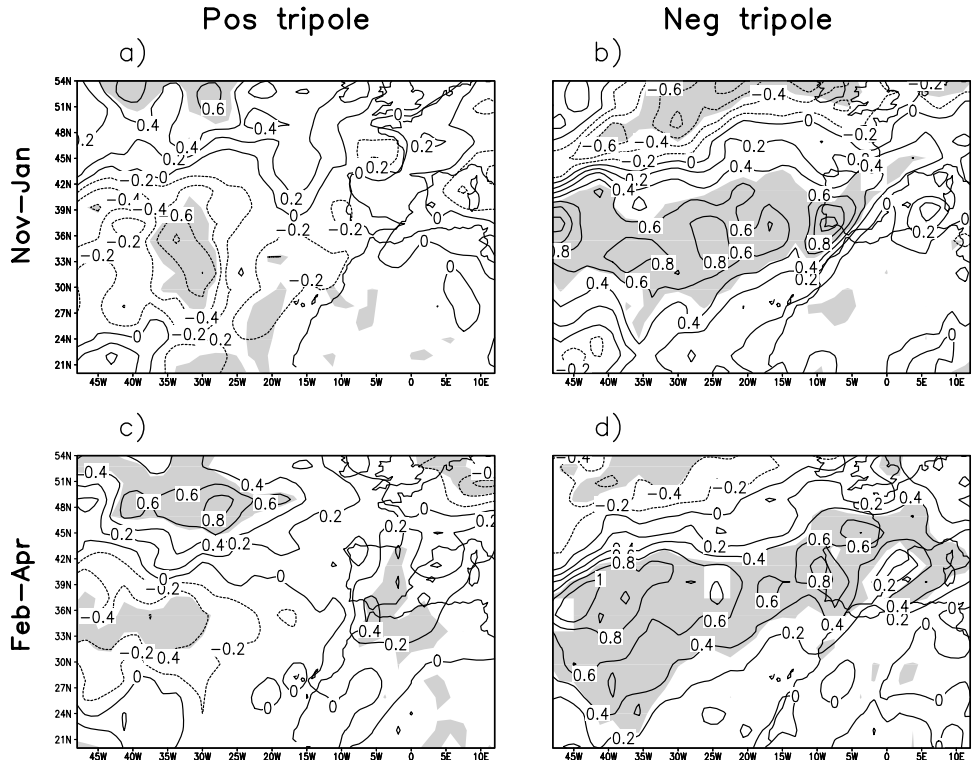

Figure 12. Composite of reanalysis precipitation (mm/day) for the months when observed SST has a strongly positive/negative projection on the SST tripole. (a) For the 48 months with strongly positive projection in early-mid winter; (b) as (a) but for the 45 months with strongly negative projection; (c) as in (a) but for the 55 months with strongly positive projection in late winter; (d) as (b) but for the 58 months with a strongly negative projection in late winter. The shading denotes areas significant at 90%, as estimated by a t-test.

negative tripole runs and the control runs is small. During the late winter months, there is more precipitation in the negative tripole runs while the difference between the control runs and the positive tripole runs is not clear. The seasonal mean rainfall association with the SST for the two seasons is similar in the monthly rainfall indices. T-tests for the significance of the seasonal differences in monthly rainfall index between the control runs and the SSTA runs are carried out for both early-mid and late winter. The results suggest that in early-mid winter, the difference between the control runs and the positive SST tripole runs is significant at the 99% level, while the difference between the control and the negative runs is not significant. In late winter, the difference between the control runs and the negative runs is significant at the 95% level, while the difference between the control runs and the positive runs is not significant. All these features are consistent with Figure 10. In the composite index of observed NW African monthly rainfall (Figure 15b), from November through February there is less rainfall for the positive tripole. This is consistent with the GCM simulations. In February, for the negative tripole there is more rainfall, which is also consistent with the GCM. Other months showed marked disagreements between the GCM and the observations. In particular, the positive tripole is associated with a strong increase in April rainfall, a result not reproduced in the simulations.

[36] For the seasonal mean observations, the positive tripole corresponds to less rainfall in early-mid winter at the 99% significance level, and the negative tripole corresponds to more rainfall in late winter, though this is barely (90%) significant. Both are consistent with the GCM simulations. For the negative tripole in early winter, there is more but not significantly more, rainfall, and for the positive tripole in late winter, there is more rainfall with again marginal significance. Neither result is found in the simulations. The observed Moroccan monthly rainfall index (Figure 15c) is generally consistent with the observed NW Africa rainfall index (Figure 15b), sharing the same months and seasons of agreement and disagreement with the simulations.

[37] These results suggest that the seasonality of the response to the tripole is not the same in the observations and in the model, but there is general agreement that the positive tripole suppresses NW African rainfall and the negative tripole enhances it. That the relationship appears stronger (albeit less significant) in the observations is not surprising. Assuming it is the NAO that induces the change in NW Africa rainfall, much of the variability in the NAO is intrinsic to the atmosphere. Thus, the relationship in the observations includes cases in which the atmosphere forces the ocean, while the model results include only the influence of the ocean on the atmosphere.

6. Summary and Discussions

[38] The influence of the North Atlantic SST tripole on NW African rainfall is explored using a large ensemble of

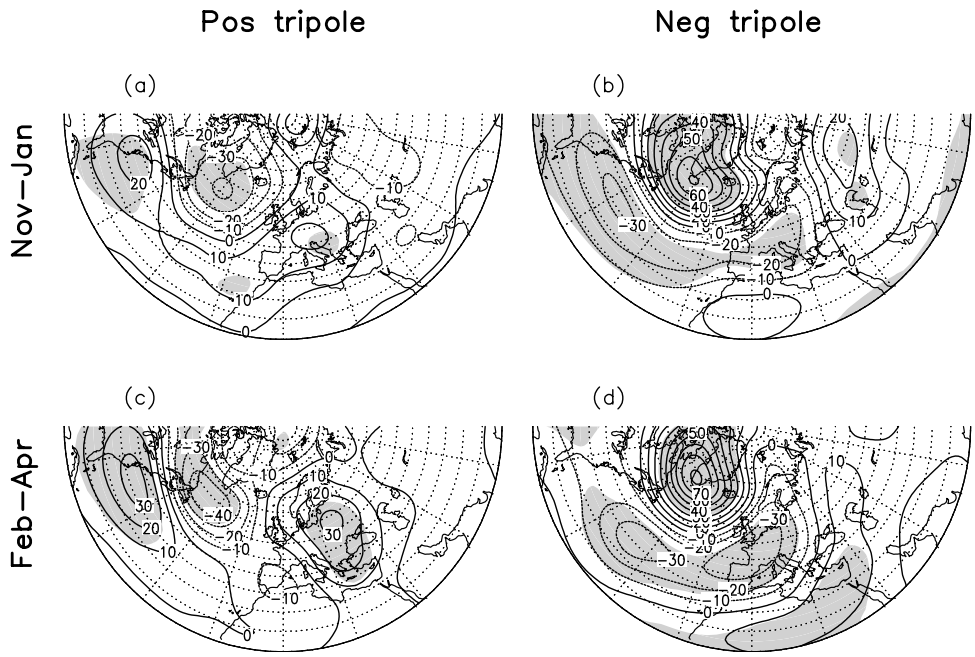

Figure 13. Same as Figure 12, but for 500 hPa geopotential height (m). The shading denotes areas significant at the level of 95%, as estimated by a t-test.

GCM experiments. It is found that this influence is nonlinear or asymmetric about the sign of the SST tripole, and is different in the early-mid and late winter. In early-mid winter (November to January), the positive SST tripole induces a negative rainfall anomaly and an increased risk of drought, while a negative SST tripole does not significantly enhance the rainfall. In late winter (February to April) the positive SST tripole does not induce significant rainfall anomalies, while the negative tripole produces a significant increase in rainfall. Further diagnoses suggest that the asymmetry and seasonal dependence of the SST influence on NW African rainfall are consistent with the asymmetric and seasonally dependent response of the large-scale atmospheric circulation in our model.

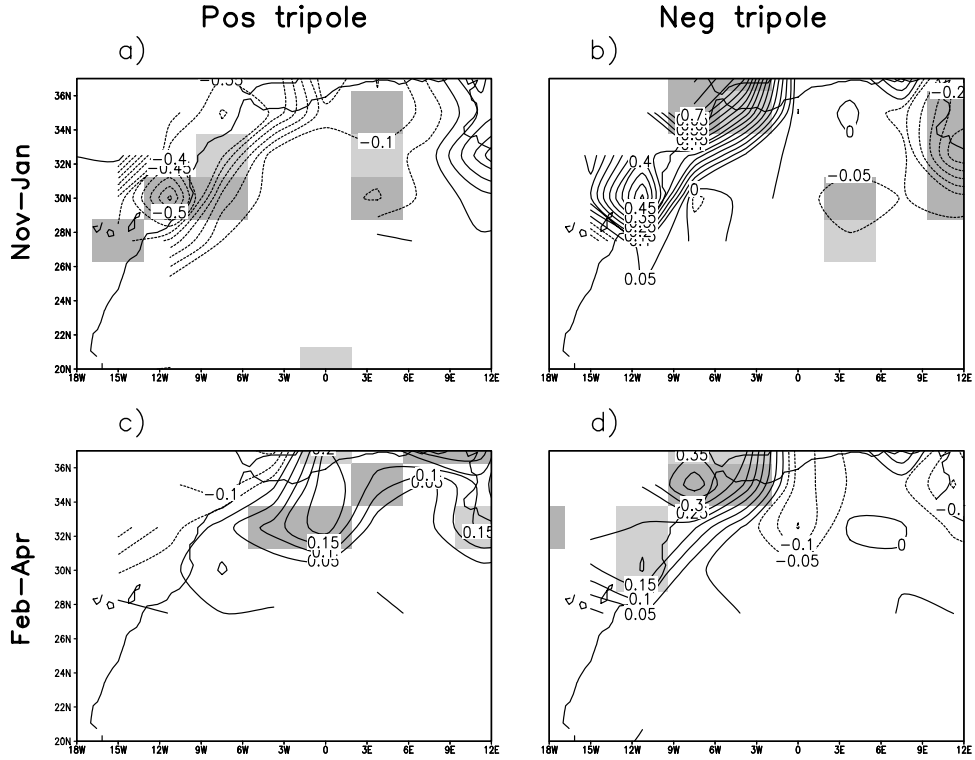

Figure 14. As in Figure 12, but using Hulme's global land-area rainfall data set instead the reanalysis.

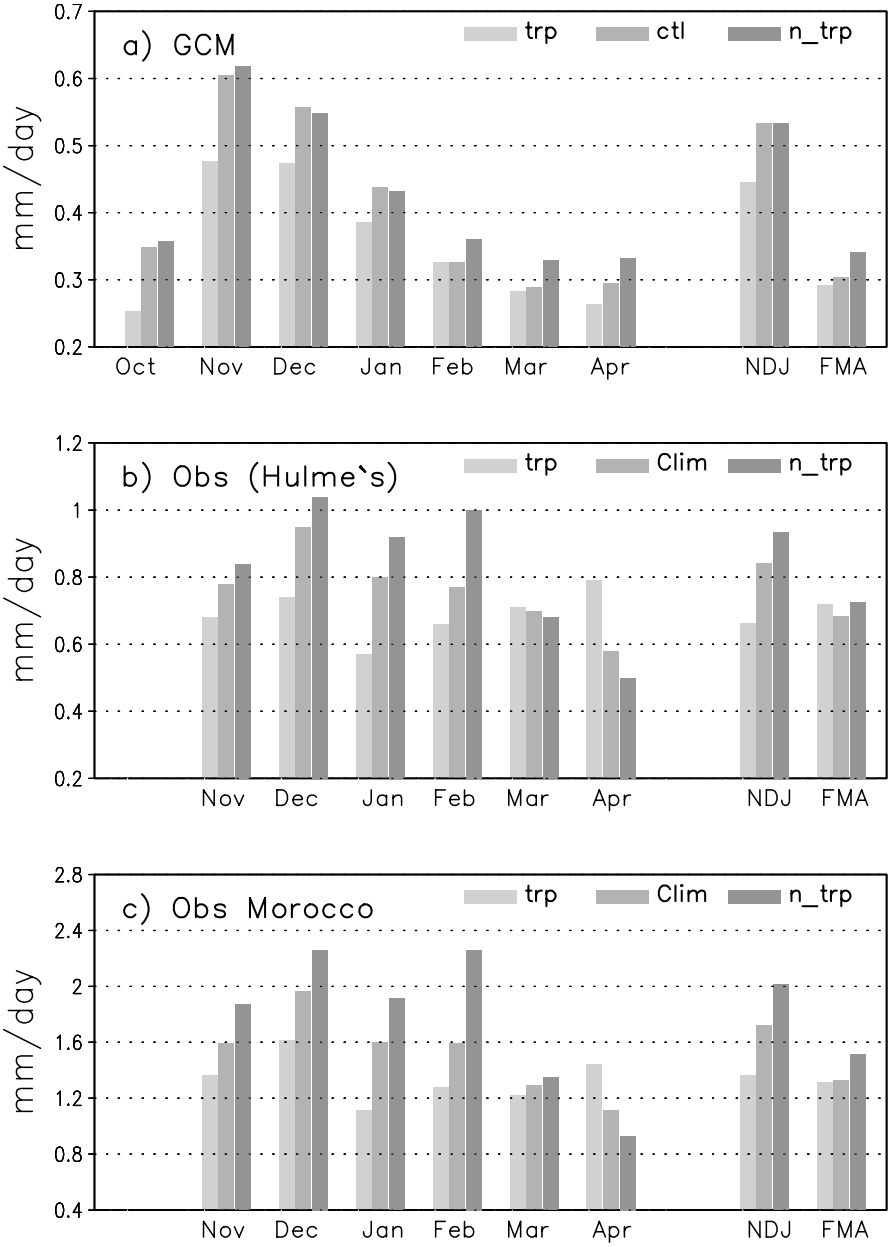

Figure 15. Northwest African monthly precipitation index in GCM (a) and in observations (b) for early-mid and late winter for the different SST. Unit: mm/day. (a) GCM control runs and the positive/negative SST tripole runs. (b) Observational climatology and the composite in Hulme's data set when observed SST has a strongly positive/negative projection on the tripole. (c) As (b), but for coastal Africa (Morocco). Unit: mm/day. In (a), "trp" indicates the SST tripole run and "n_trp" the negative SST tripole run. In (b) and (c), "clim" means climatology, "+trp"/"−trp" indicates the composite when observed SST has a strongly positive/negative projection on the SST tripole.

[39] The modeled atmospheric response that produces the strongest rainfall anomaly over the Mediterranean, that to the negative tripole in late winter, is consistent with the pattern of internal model variability that is selected by composing the wettest years in the control run (Figures 7 and 9). This supports the idea that SST anomalies induce changes in precipitation through their influence on the location of the North Atlantic jet and stormtrack, i.e., through their influence on the NAO, an internal mode of atmospheric variability.

[40] The modeled SST association with NW Africa rainfall is similar to the SST association with coastal Africa

(Morocco) rainfall in observations. The modeled asymmetry in large-scale circulation and rainfall responses to the SST in late winter is also largely consistent with observational composites. Moreover, the model captures this relationship through its large-scale atmospheric response to the SST tripole and through the response of NW African rainfall to the resulting changes in the large-scale atmospheric flow. The latter aspect of the response is consistent with the generation of rainfall anomalies by the internal variability within model, and this variability is also consistent with observations. This suggests that the observed association between the SST tripole and precipitation, results, at least in part, from an atmospheric response to the SST. If this is indeed the case, because the SST evolves more slowly than the atmospheric circulation, it raises the possibility that North Atlantic SST may be helpful for seasonal predictions of rainfall along the NW coast of Africa.

[41] There are two significant limitations to this present study. The first is an issue of spatial scale. NW African rainfall has a complicated distribution on small spatial scales, shaped, at least in part, by complex topography. For example, previous observational studies have shown a significant NAO influence only on Moroccan rainfall. Here, however, given the coarse resolution of our global model, we consider the rainfall over a broad region of NW Africa. Secondly, our model shows significantly different seasonality in its relationships between precipitation and the large-scale flow, and between the large-scale flow and SST than are found in observations. As previously noted [*Peng et al.*, 2002] our model captures the observed structure of large-scale internal atmospheric variability and, therefore, the atmospheric response to SST, in the late winter, February to April, better than in the early-mid winter, November to January. For this reason, all of the results are shown separately for these two periods. In general, the model resembles the observations better in late than in early-mid winter.

[42] Recently, *Czaja and Frankignoul* [2002] suggest that a pan-Atlantic SST anomaly, the North Atlantic horseshoe (NAH) may serve as a predictor for the SST tripole and NAO in winter (NDJ, corresponding to early-mid winter here) months in advance. They also suggest that the tropical Atlantic can influence the NAO. Some studies have shown that ENSO affects tropical Atlantic SST [*Marshall et al.*, 2001]. Based on canonical correlation analysis (CCA), *Lamb et al.* [1997] argued that tropical Pacific SSTs can be used to predict late winter (February, and especially March–April) Moroccan precipitation. Thus, further investigations of the connections of NW African rainfall with SST in many locations, including the North Atlantic, may contribute to improved seasonal forecasts of NW African rainfall.

[43] **Acknowledgments.** We are grateful to Peter Lamb and Mostafa El Hamly for providing the time series of Morocco rainfall, and to Diane Portis for her helpful comments. The suggestions from Vincent Moron and an anonymous reviewer led to significant improvements of the manuscript. This research is supported by NSF grants ATM-9902816 and ATM-9903503.

References

Cayan, D. R., Latent and sensible heat-flux anomalies over the northern oceans—Driving the sea-surface temperature, *J. Phys. Oceanogr.*, *22*, 859–881, 1992a.

Cayan, D. R., Latent and sensible heat-flux anomalies over the northern oceans—The connection to monthly atmospheric circulation, *J. Clim.*, *5*, 354–369, 1992b.

Czaja, A., and C. Frankignoul, Observed impact of Atlantic SST anomalies on the North Atlantic Oscillation, *J. Clim.*, *15*(6), 606–623, 2002.

Hulme, M., 1951–80 global land precipitation climatology for the evaluation of general circulation models, *Clim. Dyn.*, *7*, 57–72, 1992.

Hurrell, J. W., Decadal trends in the North Atlantic Oscillation: Regional temperatures and precipitation, *Science*, *269*, 676–679, 1995.

Kalnay, E., The NCEP/NCAR 40-year reanalysis project, *Bull. Am. Meteorol. Soc.*, *77*, 437–471, 1996.

Lamb, P. J., and R. A. Peppler, North Atlantic Oscillation: Concept and an application, *Bull. Am. Meteorol. Soc.*, *68*(10), 1218–1225, 1987.

Lamb, P. J., M. El Hamly, M. N. Ward, R. Sebbari, and D. H. Portis, Towards the seasonal prediction of Moroccan precipitation, paper presented at Twenty-Second Climate Diagnostics and Prediction Workshop, U.S. Dep. of Commer., Berkeley, Calif., 1997.

Marshall, J., Y. Kushnir, D. Battisti, P. Chang, A. Czaja, R. Dickson, J. Hurrell, M. McCartney, R. Saravanan, and M. Visbeck, North Atlantic climate variability: Phenomena, impacts and mechanisms, *Int. J. Climatol.*, *21*, 1863–1898, 2001.

Palmer, T. N., and Z. Sun, A modeling and observational study of the relationship between sea surface temperature in the northwest Atlantic and the atmospheric general circulation, *Q. J. R. Meteorol. Soc.*, *111*, 947–975, 1985.

Peng, S., W. A. Robinson, and S. Li, North Atlantic SST forcing of the NAO and relationships with intrinsic hemispheric variability, *Geophys. Res. Lett.*, *29*(8), 117, 2002.

Peng, S., W. A. Robinson, and S. Li, Mechanisms for the NAO responses to the North Atlantic SST tripole, *J. Clim.*, *16*, 1987–2004, 2003.

Rayner, N. A., E. B. Horton, D. E. Parker, C. K. Folland, and R. B. Hackett, Version 2.2 of the global sea surface temperature data set, 1903–1994, *Clim. Res. Tech. Note 74*, Hadley Cent. for Clim. Predict. and Res., Met Off., Bracknell, UK, 1996.

Rodwell, M. J., D. P. Rowell, and C. K. Folland, Oceanic forcing of the wintertime North Atlantic Oscillation and European climate, *Nature*, *398*, 320–323, 1999.

Rogers, J. C., The association between the North Atlantic Oscillation and the Southern Oscillation in the Northern hemisphere, *Mon. Weather Rev.*, *112*, 1999–2015, 1984.

Rogers, J. C., Patterns of low-frequency monthly sea level pressure variability (1899–1986) and associated wave cyclone frequencies, *J. Clim.*, *3*, 1364–1379, 1990.

Rogers, J. C., North Atlantic storm track variability and its association to the North Atlantic Oscillation and climate variability of northern Europe, *J. Clim.*, *10*, 1635–1647, 1997.

Sutton, R. T., W. A. Norton, and S. P. Jewson, The North Atlantic Oscillation—What role for the ocean?, *Atmos. Sci. Lett. R. Meteorol. Soc.*, Feb., 2001.

Ting, M., and N.-C. Lau, A diagnostic and modeling study of the monthly mean wintertime anomalies appearing in a 100-year GCM experiment, *J. Atmos. Sci.*, *50*, 2845–2867, 1993.

Ward, M. N., P. J. Lamb, M. El Hamly, R. Sebbari, and D. H. Portis, Climate variability in northern Africa: Understanding droughts in the Sahel and the Maghreb, in *Beyond El Niño*: *Decadal and Interdecadal Climate Variability*, edited by A. Navara, chap. 6, pp. 119–140, Springer-Verlag, New York, 1999.

Xie, P., and P. A. Arkin, Global precipitation: A 17-year monthly analysis based on gauge observations, satellite estimates and numerical model outputs, *Bull. Am. Meteorol. Soc.*, *78*, 2539–2558, 1997.

S. Li and S. Peng, NOAA-CIRES Climate Diagnostics Center, University of Colorado, R/CDC1, 325 Broadway, Boulder, CO 80305-3328, USA. (shuanglin.li@noaa.gov)

W. A. Robinson, Department of Atmospheric Sciences, University of Illinois, Urbana, IL 61801, USA.